



EXPERIMENTAL INVESTIGATION OF SEISMIC BEHAVIOR OF LIGHT-FRAMED WOOD SHEAR WALLS WITH SUPPLEMENTAL ENERGY DISSIPATION

David A. DUTIL¹ and Michael D. SYMANS²

SUMMARY

As performance-based seismic design becomes more prevalent, increasing attention is being given to improving building performance during seismic events. Much attention has been given to improving the seismic performance of steel and concrete structures, with relatively little attention having been given to woodframe buildings. Although life-safety is generally not a significant concern for woodframe buildings, the financial impact associated with the damage to such structures during strong earthquakes can be devastating. The objective of this research was to determine, through experimental testing, the suitability of supplemental fluid dampers for improving the seismic performance of wood-framed shear walls. Experimental testing of full-scale wood-framed shear walls was performed using a seismic shaking table in which in-plane excitation was applied at the base of the walls. Two different wall configurations were tested; one that employed conventional framing and another that employed a modified framing system combined with a supplemental fluid damper. The results of the shaking table tests revealed that the wall configuration that employed a supplemental fluid damper offered improved performance as compared to the conventional wall configuration in terms of reducing the peak interstory drift, peak acceleration, and inelastic energy dissipation demand on the wood framing.

INTRODUCTION

Wood-framed structures have historically performed well during seismic events and thus are regarded as having satisfied the implied performance objective of current building codes [1]. The primary reason that wood structures survive earthquakes is their ability to dissipate large amounts of energy. Unfortunately, the energy is dissipated by distortion of the framing system, inelastic action in the framing connections, and non-structural damage to gypsum board sheathing, resulting in significant financial loss associated with repair of both the structural and non-structural systems. As one example, the January 17, 1994 Northridge, CA Earthquake reinforced the need for more attention being given to the seismic performance of woodframe structures. This particular earthquake caused more than \$20 billion in property damage to

¹ Associate Engineer, Daigle Engineers, Methuen, MA. Email: ddutil@daigleengineers.com

² Associate Professor, Dept. of Civil & Env. Engineering, Rensselaer Polytechnic Institute, Troy, NY.
Email: symans@rpi.edu

woodframe structures [2]. The level of damage to such structures varied widely from small non-structural cracking in wall sheathings and personal property damage to complete collapse of the structure. The CUREE report entitled *Woodframe Project Case Studies* [2] documents observations of damage and failures in wood-framed structures caused by the Northridge Earthquake. Many of the structures examined suffered damage due to either failure of lateral force resisting shear walls, failure of a soft story, design or construction errors, or soil failure. The latter is a condition that cannot be improved upon structurally whereas the other three can. For example, by including a supplemental seismic damper in the structure, the components of the structure will not be required to dissipate all of the seismic input energy. Instead, the damper would dissipate a large portion of the seismic input energy. The reduced demand on the structural elements could improve the survivability of shear walls, reduce the displacement and thus improve the performance of soft stories, and perhaps even offset some design or construction errors, thereby improving the performance of wood-framed structures. In recent years, research has taken place to explore the possibility of introducing supplemental energy dissipation devices into woodframe construction.

Filiatrault [3] performed numerical studies on the seismic response of wood shear walls with friction dampers located in the four corners of the wall. Dinehart and Shenton [4] and Dinehart et al. [1] experimentally evaluated four different damper arrangements in woodframe shear walls wherein the dampers employed shearing action of a viscoelastic material to dissipate energy. In addition, Dinehart and Lewicki [5] experimentally tested a woodframe shear wall with a thin layer of VE material between the sheathing and the studs. Cyclic testing was carried out by Higgins [6] on a wood shear wall containing a kinematically expanding hysteretic damper wherein energy dissipation occurs via yielding of a mild steel rod oriented along the diagonal of the wall. Symans et al. [7] numerically evaluated the seismic performance of woodframe shear walls and building frames with fluid dampers. Non-linear finite element analyses were performed using a linear fluid viscous damper within the shear walls.

The results from the numerical and experimental studies referred to above demonstrate that the inclusion of supplemental dampers in woodframed shear walls is effective in increasing either or both the stiffness and energy dissipation capacity of the wall/damper system. Furthermore, the dampers provide a non-degradable source of energy dissipation over repeated cycles of motion and typically increase the size of the hysteresis loops near the zero displacement position (i.e., the position at which the woodframed shear wall offers minimal lateral force resistance due to its characteristic pinching response). Finally, in some cases the dampers provide additional stability to the shear wall due to either their orientation in the wall or their inherent restoring force characteristics.

With regard to fluid dampers, it is evident that they have significant potential for application within the relatively narrow confines of woodframed shear walls due to their high-energy dissipation density (i.e., high energy dissipation capacity per unit volume). Furthermore, the results from the numerical analyses performed by Symans et al. [7] clearly demonstrate the potentially significant benefits of fluid dampers for seismic energy dissipation in wood shear walls. In an attempt to validate the general findings obtained in the numerical study by Symans et al. [7], the research contained herein experimentally examines the behavior of a wood-framed shear wall subjected to earthquake loading via a seismic shaking table.

EXPERIMENTAL TEST SETUP AND SEISMIC EXCITATION

Construction of Test Walls

Six test walls were constructed in accordance with the 2000 International Building Code (2000 IBC) [8] and tested on a seismic shaking table with the shaking table motion applied along the in-plane direction of the wall. Four of the test walls were constructed in a conventional configuration and two were constructed in a modified configuration to allow for a fluid viscous damper and required attachment hardware to be

installed inside the wall. All six walls were designed, constructed, and loaded to simulate the first-story wall in a two-story wood-framed residential structure. Each of the conventional walls was provided with two hold-downs and two anchor bolts (see Figure 1a) whereas each of the retrofitted walls was provided with two hold-downs and one anchor bolt (see Figure 1b). The difference in the number of anchor bolts was due to the interference of the installed damper hardware within the retrofitted walls.

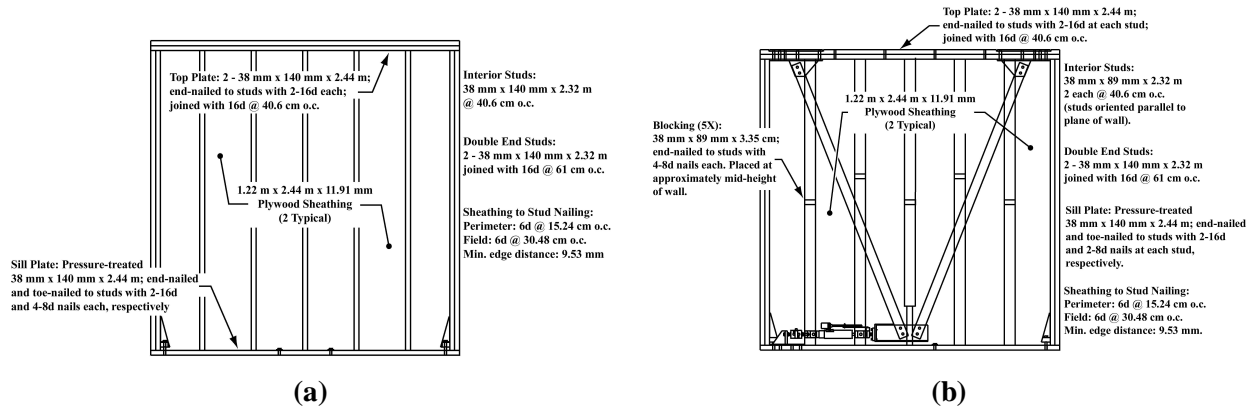


Figure 1 – Construction of (a) Conventional and (b) Retrofitted Wood-Frame Shear Wall

The conventional wood shear walls were 2.44 m x 2.44 m (8 ft x 8 ft) and were framed with 38 mm x 140 mm (2 in. x 6 in. nominal) Spruce-Pine-Fir (SPF) interior studs spaced at 40.64 cm (16 in.) on center. The studs were oriented perpendicular to the plane of the wall. Double end studs and a double top plate were used. The sill plate was a 38 mm x 140 mm (2 in. x 6 in. nominal) pressure-treated member. The wall was sheathed on one side with two 1.22 m x 2.44 m x 11.91 mm thick (4 ft x 8 ft x 15/32 in. thick) plywood sheathing panels oriented vertically. The nailing schedule was in accordance with the 2000 IBC. In particular, the plywood sheathing panels were nailed to the framing members using 6d common nails with a perimeter spacing of 15.24 cm (6 in.) and a field spacing of 30.48 cm (12 in.). According to the 2000 IBC, if 38 mm x 140 mm (2 in. x 6 in. nominal) studs are used in the construction of a wall supporting one floor, roof, and ceiling, the spacing of the studs shall be 60.96 cm (24 in.) on center. However, a spacing of 40.64 cm (16 in.) was used for the conventional wall test specimens so as to maintain consistency with the spacing that was used in the retrofitted wall.

The retrofitted wood shear walls were 2.44 m x 2.44 m (8 ft x 8 ft) and framed using both 38 mm x 89 mm (2 in. x 4 in. nominal) and 38 mm x 140 mm (2 in. x 6 in. nominal) SPF studs. The 38 mm x 140 mm (2 in. x 6 in. nominal) members were used for the double end studs and double top plate. These members were oriented perpendicular to the plane of the wall. The 38 mm x 89 mm (2 in. x 4 in. nominal) members were used for the interior studs spaced at 40.6 cm (16 in.) on center. At each 40.6 cm (16 in.) interval, two studs were placed. These studs were oriented parallel to the plane of the wall with one of the long sides of the stud placed flush to the outside of the wall so that the space between the two studs was 6.35 cm (2.5 in.). This space was used to accommodate a fluid viscous damper and the required damper attachment hardware. The bottom 30.5 cm (12 in.) of the two center studs were notched to allow motion of the bottom of the inverted chevron brace in the plane of the wall. Horizontal blocking was placed between each pair of 38 mm x 89 mm (2 in. x 4 in. nominal) studs at the approximate mid-height of the wall. The blocking prevented the possibility of weak axis buckling of the studs. The vertical position of the blocking was adjusted in two locations to prevent interference with the damper connection hardware. The sill plate was a 38 mm x 140 mm (2 in. x 6 in. nominal) pressure-treated member. The wall was sheathed on one side with two 1.22 m x 2.44 m x 11.91 mm thick (4 ft x 8 ft x 15/32 in. thick) plywood sheathing panels oriented vertically. The nailing schedule for the retrofitted wall was identical to that of the conventional wall with the exception of the blocking, which did not exist in the conventional wall, and the toe-nailing

of the interior studs to the sill plate. Details on the installation of the fluid viscous damper will be discussed subsequently.

Gravity Loading

The test specimens were designed to represent load-bearing first-story walls in a two-story wood-framed residential structure. A distributed load was applied to the top of the wall to simulate 21.24 kN (4,776 lbs) [or 8.71 kN/m (597 lb/ft)] of gravity loading. The load was applied to the wall via a 2.74 m (9 ft) long W14x120 wide-flanged steel beam that was attached to the double top plate of the wall. The beam was oriented with its web horizontal and lead bricks were positioned between the two vertical flanges to increase the load beyond the beam self-weight. The combination of the steel beam and lead bricks is referred to herein as the *load beam*.

Shear Wall Lateral Support System

As constructed, the wall test specimens were laterally unstable in the out-of-plane direction. In addition, torsional modes of vibration were expected since the center of mass and center of stiffness of the wall did not coincide. To minimize out-of-plane motion of the wall, a lateral support frame was constructed and mounted to the main support beams of the shaking table. The frame provided out-of-plane support to the load beam and therefore to the top of the wall. The support was provided by two hard rubber casters mounted to the lateral support frame on each side of the load beam. The casters were in contact with the sides of the load beam to restrain the beam from any translation or rotation out of the plane of the wall. Each caster was positioned so that the rolling action of the caster was in the direction of motion of the plane of the wall so as to minimize the resistance to in-plane motion of the wall.

Sensors and Instrumentation

Seven sensors were used to measure the dynamic response of the conventional wall test specimens. These included two displacement/velocity transducers and five accelerometers. Two additional sensors, a load cell and displacement/velocity transducer, were utilized to measure the response of the fluid damper in the retrofitted wall. The signals from each of the sensors were conditioned, multiplexed, and recorded using a PC-based data acquisition (DAQ) system running LabVIEW 7.0. The DAQ system had maximum acquisition and output rates of 333,000 samples per second. In addition to data acquisition, the LabVIEW program was used to provide an output signal to the shaking table servo-controller.

Seismic Excitation

The shear walls were subjected to two distinct types of earthquake ground motion via the seismic shaking table. Seismic Loading I was an Ordinary (a.k.a. far-field) Ground Motion (OGM) record. For this loading, the S16W component of the ground motion recorded during the 1994 Northridge Earthquake at 7769 Topanga Canyon Blvd., Canoga Park, CA was selected. Seismic Loading II was a Near-Field Ground Motion (NGM) record. For this loading, the S49W component of the ground motion recorded during the 1994 Northridge Earthquake at the Rinaldi Receiving Station was selected. Note that these two ground motion records are the same as those used by Fischer et al. [9] for shaking table tests of a two-story woodframe house. The peak ground acceleration, velocity, and displacement of the OGM record are 0.389 g, 59.8 cm/sec, and 12.4 cm, respectively, and, for the NGM record, the respective values are 0.842 g, 170.3 cm/sec, and 33.4 cm. The displacement capacity of the seismic shaking table was sufficient to permit 100 percent and 38 percent of the OGM and NGM records, respectively, to be applied to the shear walls. As expected, an examination of the Fourier amplitude spectra for the OGM and NGM records reveals that the NGM clearly exhibits stronger components at all frequencies and particularly at low frequencies.

DESCRIPTION OF FLUID DAMPER AND INSTALLATION

The supplemental seismic damper used in the experimental tests was a fluid viscous damper which was selected due to its high energy dissipation density (i.e., its ability to dissipate significant amounts of energy in comparison to its physical size). The compact size of the damper allowed for convenient placement of the damper within the confines of a wood-framed shear wall. The basic damper configuration was identical to the dampers that were utilized for seismic protection of the Ataturk Airport in Istanbul, Turkey. The damper consisted of two major parts, a cylinder and a piston rod, and was constructed in a through-rod configuration (see Figure 2). The cylinder was filled with a silicone fluid having a kinematic viscosity of 1,000 centistokes at an ambient temperature of 20°C (68°F). Inside the larger, hollow cylinder that makes up the main body of the damper, a thin cylinder containing small orifices was attached to the piston rod. As the damper was stroked, the silicone fluid was forced to pass through the orifices at a high speed. This action generated heat energy that was released to the environment.

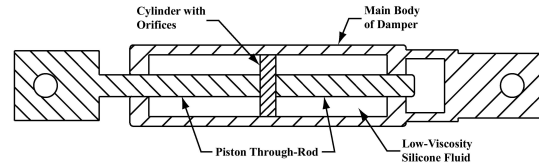


Figure 2 – Cut-Away View of Fluid Viscous Damper with through-rod configuration.

The damper used in the experimental tests weighed 57.8 N (13 lbf), had a stroke capacity of ± 2.54 cm (± 1 in.), and had a rated force capacity of 44.47 kN (10 kips). It was designed to produce a force that varied linearly with velocity such that at the design velocity of 25.4 cm/sec (10 in./sec), a force of 13.34 kN (3 kips) was required to stroke the damper. Thus the design damping coefficient, C_D , was 525.4 N-sec/cm (300 lbf-sec/in). Experimental data from three different cyclic tests revealed that over a frequency range of 0 to 2 Hz, the damper behaves essentially as a linear viscous dashpot. Since the damper has a run-through rod configuration, it is expected that the damper would develop minimal stiffness at higher frequencies and thus would continue to behave as a linear viscous dashpot at frequencies beyond 2 Hz.

Prior to cyclic testing of the damper, application of static loads to the damper revealed that the static friction force was approximately 312 N (70 lbf) which represents approximately 0.7% of the rated force capacity of the damper. The friction force develops at each end of the damper at the interface between the piston rod and the piston rod seals. During seismic testing of the retrofitted shear wall, the maximum damper force exceeded the static friction force by a factor of about 13 and 8 for Seismic Loading I and II, respectively.

As shown in Figure 3, the damper was installed in an inverted chevron brace configuration. This arrangement offered two main advantages over other configurations considered – simplicity and direct transfer of lateral motion to the damper. In a design where the damper would have been connected to the top of the wall via a diagonal brace, the motion activating the damper would be a component of the horizontal motion of the wall. In contrast, the inverted chevron brace configuration directly transfers the horizontal motion of the top of the wall to the damper. This direct transfer cycles the damper more effectively, allowing more energy to be dissipated by the damper. In addition, fabrication and installation of the connection hardware for the inverted chevron brace configuration were relatively simple compared to other configurations that were considered. The simplicity of fabrication and installation is important since implementation in practice must be both feasible and cost effective.

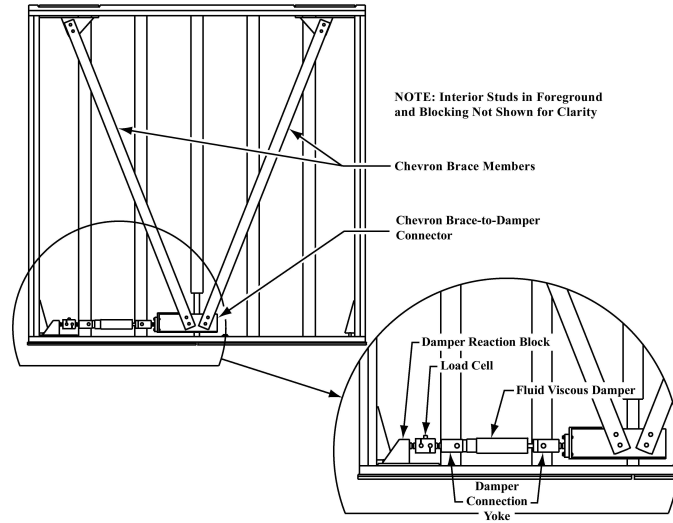


Figure 3 – Installation of Fluid Viscous Damper within Wood-Framed Shear Wall

SYSTEM IDENTIFICATION OF SHEAR WALLS

As shown in Table 1, a total of six walls, four conventional and two retrofitted, were experimentally tested. Each wall was excited with white noise to identify the dynamic characteristics of the wall and then with earthquake ground motions to evaluate the seismic response of the wall. The first two conventional walls were pre-test walls that were used to identify any problems with the test set-up and to provide preliminary seismic response data.

Table 1 – Description of Test Walls Used in Experimental Test Program

| Test Wall # | Configuration (Stud Spacing) | Seismic Loading |
|--------------------|-------------------------------------|------------------------|
| Pre-Test I | Conventional (60.96 cm) | OGM and NGM |
| Pre-Test II | Conventional (40.64 cm) | OGM |
| I | Conventional (40.64 cm) | OGM |
| II | Conventional (40.64 cm) | NGM |
| III | Retrofitted (40.64 cm) | OGM |
| IV | Retrofitted (40.64 cm) | NGM |

System identification tests were performed both before and after each test specimen was subjected to earthquake ground motion. The system identification tests were performed using low-amplitude white noise excitation as input at the base of the wall. The response of the wall for such low amplitude excitation was expected to be elastic and to therefore cause minimal strength degradation prior to seismic testing. Accordingly, for system identification purposes, it was assumed that the shear wall could be modeled as a single-degree-of-freedom (SDOF) system with linear elastic stiffness and linear viscous

damping. For each test wall, the white noise excitation had a uniform power spectral density with a frequency content of 0 to 30 Hz and a maximum amplitude of ± 0.51 mm (± 0.02 in.).

Time- and Frequency-Domain System Identification Methods

The recorded accelerations at the bottom and top of the wall were used to identify the natural frequency and equivalent viscous damping ratio of each wall using two different system identification methods. The first method was a time-domain method that utilized the free-vibration response of the wall after the white noise excitation stopped. From the free-vibration acceleration response of the top of the wall (see Figure 4), the natural frequency and damping ratio were estimated from the time elapsed and decay in amplitude, respectively, between two well-defined peaks of complete cycles of free vibration. The second approach that was used to identify the dynamic properties of the test walls was a frequency-domain method in which the transfer function relating the acceleration at the top and bottom of the test wall during the white noise excitation was utilized (see Figure 5). The natural frequency and damping ratio were estimated from the location and height, respectively, of the dominant peak in the amplitude of the transfer function.

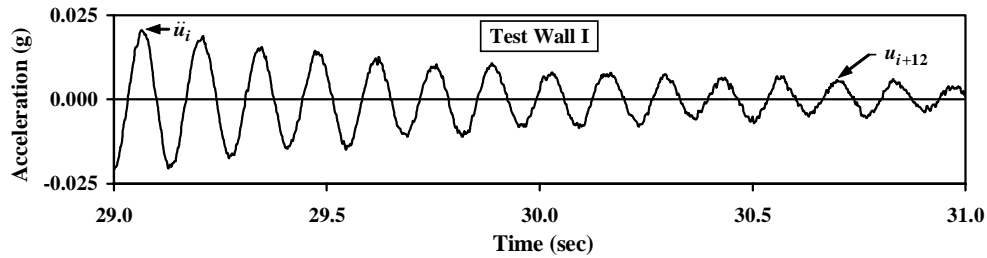


Figure 4 – Free Vibration Response of Test Wall I Prior to Seismic Excitation (Test 81)

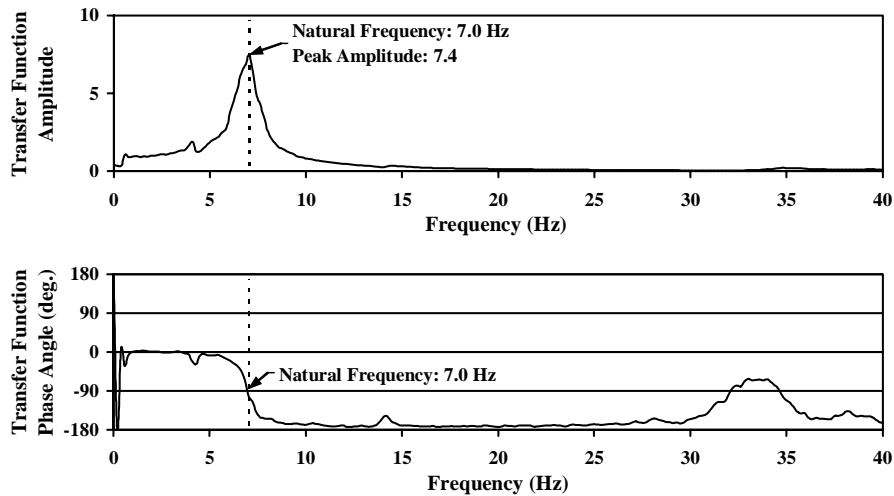


Figure 5 – Experimental Transfer Function of Test Wall I Obtained Prior to Seismic Excitation (Test 81)

Evaluation of Identified Dynamic Properties

The identified dynamic properties for Test Wall I are summarized in Figure 6 along with results for the other three test walls. The data in Figure 6 indicate that the two methods of system identification yield estimates of the natural frequency that are in reasonably close agreement whereas the damping ratio estimates can be significantly different with the estimate from the transfer function amplitude being

consistently higher than that from the free-vibration response. The large difference in the estimates of the damping ratios is likely due to the inability to accurately identify the maximum amplitude of the transfer function. For low levels of damping, the value of the amplitude of the transfer function varies rapidly at frequencies near the natural frequency and its value tends to be underestimated due to the discretized nature of the transfer function data. Thus, the damping ratios that are estimated from the free vibration response are considered to be more accurate than those from the transfer function amplitudes.

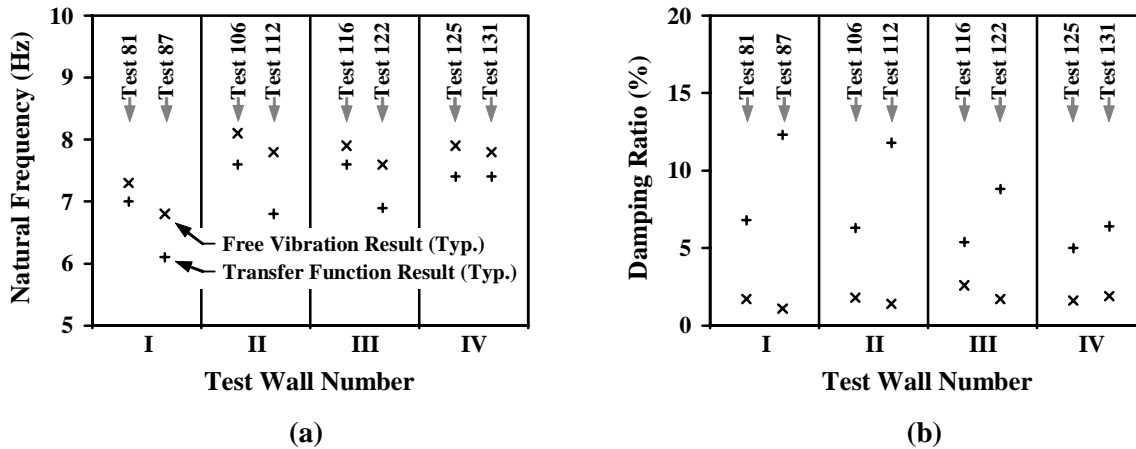


Figure 6 – Dynamic Properties of Test Walls Before and After Seismic Excitation

The dynamic properties of Test Walls I-IV were estimated before and after seismic excitation was applied to each wall. Specifically, for each test wall, the seismic excitation was repeated three times, with system identification testing performed before (lower test number for each wall in Figure 6) and after the series of three seismic excitations (higher test number for each wall in Figure 6). The purpose of subjecting each wall to three seismic events was to evaluate the wall performance when in a virgin condition and when in a damaged condition (which might occur, for example, if the wall is not repaired prior to an aftershock or another earthquake). The general trends in the data of Figure 6 are consistent with what was expected. As the test walls are cycled, the strength and stiffness of the walls tends to degrade and thus the walls become more flexible as indicated by the lower natural frequencies after the series of seismic excitations are applied (see Figure 6a). Note that the inclusion of dampers in the retrofitted walls is not expected to influence the natural frequency since the dampers behave essentially as linear viscous dashpots and thus do not add stiffness to the wall. Focusing on the damping ratios from the free-vibration response, the estimated values are approximately equal before and after the series of seismic excitations are applied (see Figure 6b). This is likely due to the fact that the system identification testing was performed at low amplitudes and thus the walls remained elastic during these tests, albeit with different elastic stiffness before and after the seismic excitations were applied.

Interestingly, the damping ratio of the retrofitted wall as measured from the free vibration response is approximately equal to that of the conventional wall (see Figure 6b). As stated previously, the free vibration response occurred at low amplitudes of vibration (less than 0.77 mm of peak interstory drift for all Test Walls). At such low amplitudes of vibration, the small amount of slack in the damper connection hardware was not entirely taken up and thus the damper was not stroked significantly. Had the damper been fully engaged during the free vibration response, the damping ratio would have been much higher – on the order of 27%. Clearly, the damping ratio measured during the free vibration response of the retrofitted walls may be regarded as being associated only with the wood structural framing system.

ENERGY-BASED EVALUATION OF SEISMIC RESPONSE

The dynamic response of the walls may be evaluated by considering the energy distribution within the wall during the seismic excitation. The energy balance for the conventional test walls may be written as [10]:

$$E_K(t) + E_V(t) + E_E(t) + E_H(t) = E_I(t) \quad (1)$$

where E_K is the kinetic energy of the load beam, E_V is the energy dissipated via rate-dependent viscous damping forces in the wall, E_E is the elastic strain energy stored in the wall, E_H is the hysteretic energy that includes inelastic strain energy and energy dissipation due to any other forms of rate-independent damping mechanisms (e.g., friction forces), and E_I is the seismic input energy from the ground motion. Note that the explicit dependence on time, t , is shown in Eq. 1. The energy terms in Eq. 1 can be determined via integration of the equation of motion (i.e., the force balance) over the relative displacement (interstory drift) of the wall. For an idealized SDOF representation of the shear wall (i.e., lumped mass, linear viscous damper, and nonlinear spring), the force balance may be written as:

$$m\ddot{u} + c\dot{u} + P_r = -m\ddot{u}_g \quad (2)$$

where m is the mass of the load beam, c is the viscous damping coefficient of the wall, P_r is the nonlinear rate-independent restoring force in the wall, u is the relative displacement of the mass with respect to the ground, \ddot{u}_g is the earthquake ground acceleration, and the overdots indicate ordinary differentiation with respect to time [10]. The energy terms in Eq. 1 can now be obtained via integration of Eq. 2 over the relative displacement of the wall. The results are as follows:

$$E_K(t) = \frac{1}{2}m\dot{u}^2 \quad E_V(t) = \int_0^t c\dot{u}^2 dt \quad E_E(t) = \frac{1}{2} \frac{P_r^2}{k} \quad E_I(t) = -\int_0^t m\ddot{u}_g \dot{u} dt \quad (3)$$

where k is the initial elastic stiffness of the wall. The elastic strain energy requires knowledge of the nonlinear restoring force, P_r , which may be computed from Eq. 2 as the negative of the sum of the base shear and viscous damping force. Note that, while the hysteretic energy dissipation, E_H , cannot be determined directly, it can be obtained by rearranging Eq. 1 and substituting in the results of Eq. 3.

Computation of the viscous damping energy and elastic strain energy requires values of the viscous damping coefficient and the elastic stiffness. These values can be estimated using the results from the low-amplitude system identification tests presented in Figure 6. Specifically, the identified properties from the free vibration response of the walls, before they were subjected to seismic excitation, were used. The average value of the natural frequency and damping ratio from these tests is 7.8 Hz and 1.9%, respectively. Using the mass of the load beam, the estimated values of the viscous damping coefficient and elastic stiffness are 40.3 N-s/cm (23.0 lbf-s/in) and 52.1 kN/cm (29.7 k/in), respectively.

Using an idealized SDOF representation, the force balance for the retrofitted shear wall may be written as

$$m\ddot{u} + c\dot{u} + C_D\dot{u} + P_r = -m\ddot{u}_g \quad (4)$$

where C_D is the viscous damping coefficient of the linear viscous supplemental damper. The energy distribution within the retrofitted shear wall is obtained by integrating Eq. 4 over the relative displacement of the wall. The resulting energy balance may be written as [10]:

$$E_K(t) + E_V(t) + E_D(t) + E_E(t) + E_H(t) = E_I(t) \quad (5)$$

where E_D is the viscous damping energy from the supplemental damper, which may be written as

$$E_D(t) = \int_0^t C_D \dot{u}^2 dt \quad (6)$$

RESULTS AND DISCUSSION

Ordinary Ground Motion

For Seismic Loading I (Ordinary Ground Motion), the seismic response of the retrofitted shear wall (Test Wall III) was significantly better than that of the conventional wall (Test Wall I). For example, the hysteresis loops for the retrofitted wall (Figure 7c and 7d) exhibit smaller maximum forces, smaller maximum interstory drifts, and smaller hysteretic energy dissipation demand as compared to the conventional wall (Figure 7a and 7b). For the first application of the seismic loading (Figure 7a and 7c), the conventional wall experienced a maximum interstory drift ratio of 0.59% while the retrofitted wall experienced a maximum drift ratio of 0.29% (i.e., retrofitting of the wall resulted in a 51.8% reduction in the interstory drift demand). For the third application of the seismic loading (Figure 7b and 7d), the conventional wall experienced a maximum interstory drift ratio of 0.91% while the retrofitted wall experienced a maximum drift ratio of 0.33% (i.e., retrofitting of the wall resulted in a 63.2% reduction in the interstory drift demand). Thus, the damper appears to be more effective in reducing the interstory drift of a shear wall that has been subjected to previous seismic excitation. In addition, a comparison of Figures 7b and 7d reveals that the conventional wall experienced appreciable inelastic response (as indicated by the pinched shape of the hysteresis loop) while the retrofitted wall did not.

As is evident in Figure 7, the increase in interstory drift from the first application of the seismic excitation to the third application is less for the retrofitted wall as compared to the conventional wall. Specifically, the conventional wall experienced an increase in interstory drift of 53.1% while the retrofitted wall experienced an increase of only 13.8%. Thus, the dampers are effective in controlling the interstory drift demand in shear walls subjected to multiple seismic excitations (e.g., shear walls subjected to strong aftershocks).

A comparison of the energy distribution within the conventional shear wall (Test Wall I) and retrofitted shear wall (Test Wall III) clearly demonstrates the reduced hysteretic energy dissipation demand on the wood framing system for the retrofitted wall (see Figure 8). As shown in Figure 8a, for the first application of the Ordinary Ground Motion, the total hysteretic energy dissipation demand on the wood framing system for the conventional wall is 0.77 kN-m. In contrast, for the retrofitted wall (see Figure 8c), the total hysteretic energy dissipation demand on the wood framing system is only 0.22 kN-m, a reduction of 71.4%. As shown in Figure 8b, for the third application of the Ordinary Ground Motion, the total hysteretic energy dissipation demand on the wood framing system for the conventional wall is 0.93 kN-m. In contrast, for the retrofitted wall (see Figure 8d), the total hysteretic energy dissipation demand on the wood framing system is only 0.20 kN-m, a reduction of 78.5%. The significant reductions in hysteretic energy dissipation demand on the wood framing system of the retrofitted wall is the direct result of the

energy dissipation provided by the fluid damper. Specifically, the fluid damper dissipates approximately 50% of the seismic input energy (see Figures 8c and 8d). Note that the kinetic and elastic strain energies are not shown in Figure 8. Although both of these quantities were computed, they were insignificant with respect to the other energy quantities and thus are not included in the figure.

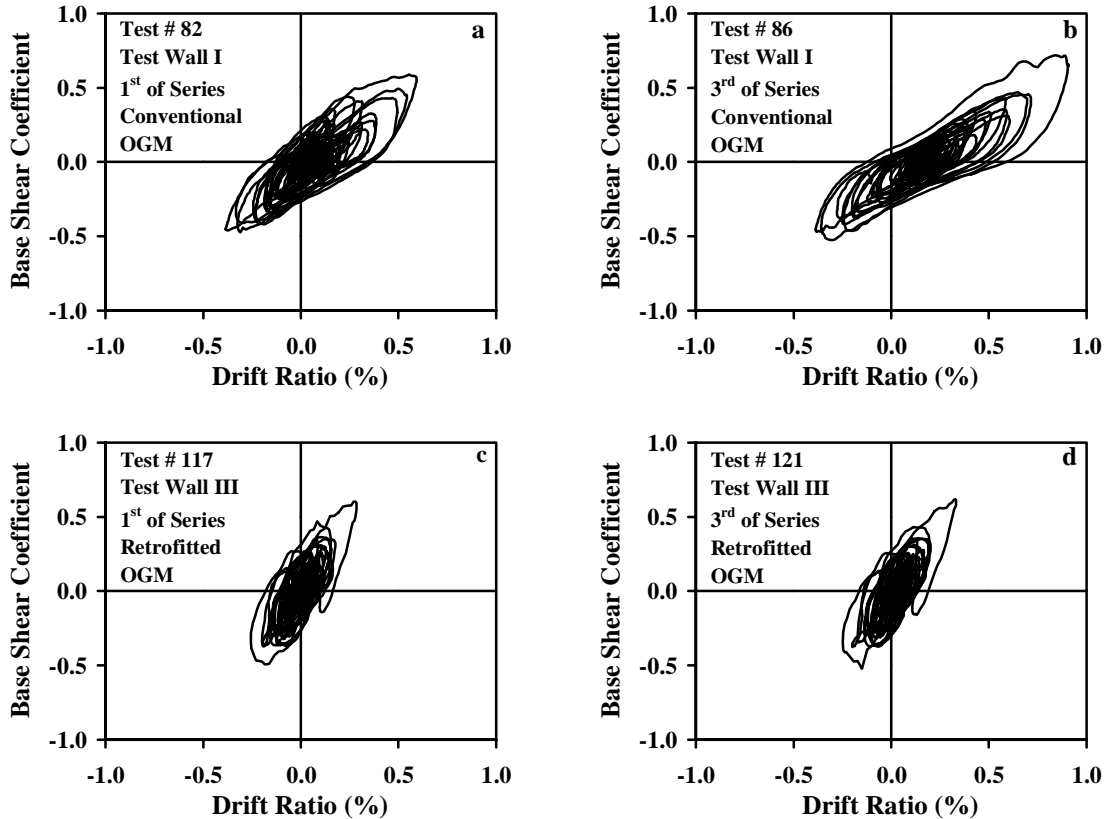


Figure 7 – Hysteresis Loops of Conventional and Retrofitted Walls Subjected to Seismic Loading I

Near-Field Ground Motion

The hysteresis loops for the conventional and retrofitted shear walls subjected to the Near-Field Ground Motion (Seismic Loading II) are shown in Figure 9. Although the maximum interstory drift of the retrofitted shear wall (Test Wall IV) is reduced as compared to the conventional shear wall (Test Wall II), the damper was not as effective as in the case of the Ordinary Ground Motion (compare Figures 7 and 9). The reduced effectiveness may be attributed to the lower seismic energy dissipation demand on the test walls subjected to the Near-Field Ground Motion, resulting in reduced stroking of the damper. Although one might expect the Near-Field Ground Motion to produce larger seismic energy dissipation demand than the Ordinary Ground Motion, this is not the case since, due to the limited displacement capacity of the shaking table, only 35% of the Near-Field Ground Motion was utilized whereas 100% of the Ordinary Ground Motion was utilized.

For the first application of the Near-Field Ground Motion (Figure 9a and 9c), the conventional wall experienced a maximum interstory drift ratio of 0.26% while the retrofitted wall experienced a maximum drift ratio of 0.20% (i.e., retrofitting of the wall resulted in a 22.5% reduction in the interstory drift). For the third application of the seismic loading (Figure 9b and 9d), the conventional wall experienced a maximum interstory drift ratio of 0.38% while the retrofitted wall experienced a maximum drift ratio of 0.22% (i.e., retrofitting of the wall resulted in a 40.8% reduction in the interstory drift). Thus, as was the

case for the Ordinary Ground Motion, the damper appears to be more effective in reducing the interstory drift of a shear wall that has been subjected to previous seismic excitation.

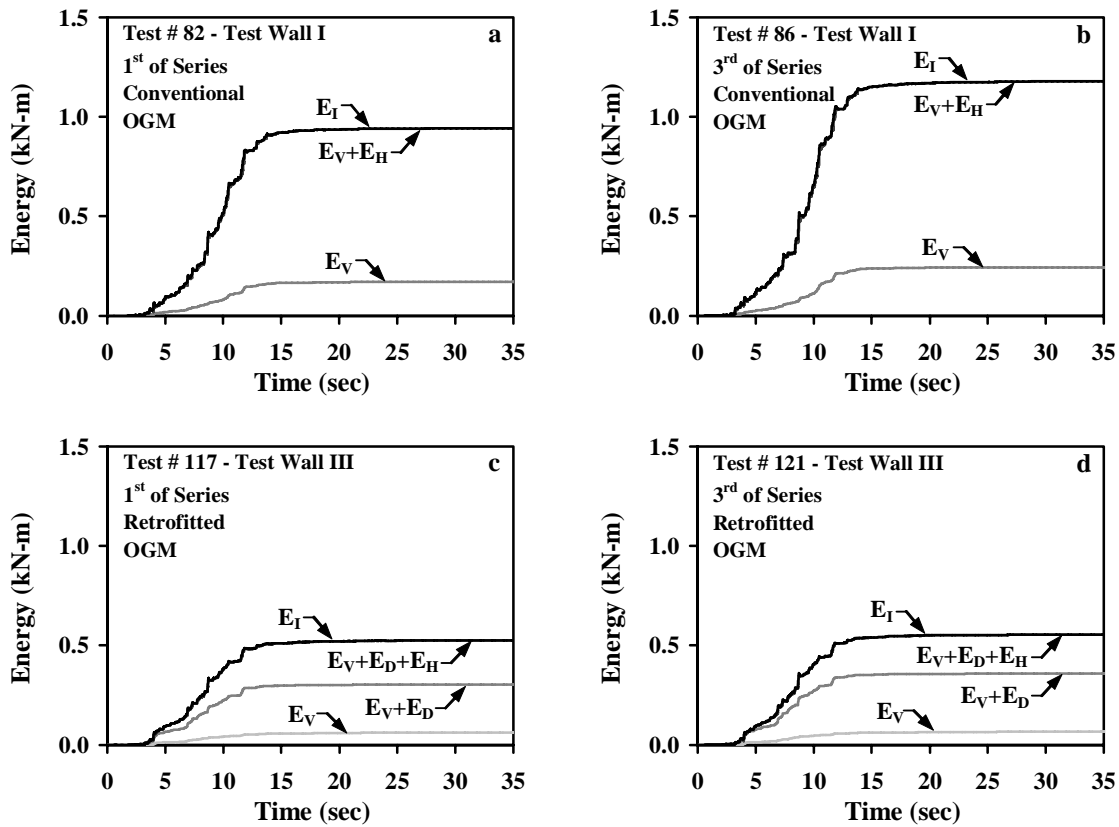


Figure 8 – Energy Distribution in Conventional and Retrofitted Walls Subjected to Ordinary Ground Motion (Seismic Loading I)

As is evident in Figure 9, the increase in interstory drift from the first application of the seismic excitation to the third application is less for the retrofitted wall as compared to the conventional wall. Specifically, the conventional wall experienced an increase in interstory drift of 44.3% while the retrofitted wall experienced an increase of 10.3%. Thus, as was the case for the Ordinary Ground Motion, the dampers are effective in controlling the interstory drift demand in shear walls subjected to multiple seismic excitations (e.g., shear walls subjected to strong aftershocks).

As for the case of the Ordinary Ground Motion, a comparison of the energy distribution within the conventional (Test Wall II) and retrofitted (Test Wall IV) demonstrates the reduced hysteretic energy dissipation demand on the wood framing system for the retrofitted wall. For the first application of the Near-Field Ground Motion, the total hysteretic energy dissipation demand on the wood framing system for the conventional wall was 0.16 kN-m. In contrast, for the retrofitted wall, the total hysteretic energy dissipation demand on the wood framing system was only 0.08 kN-m, a reduction of 50%. For the third application of the Near-Field Ground Motion, the total hysteretic energy dissipation demand on the wood framing system for the conventional wall was 0.17 kN-m. In contrast, for the retrofitted wall, the total hysteretic energy dissipation demand on the wood framing system was only 0.08 kN-m, a reduction of 52.9%. The significant reductions in hysteretic energy dissipation demand on the wood framing system of the retrofitted wall is the direct result of the energy dissipation provided by the fluid damper. Specifically,

for the Near-Field Ground Motion, the fluid damper dissipated approximately 25% of the seismic input energy.

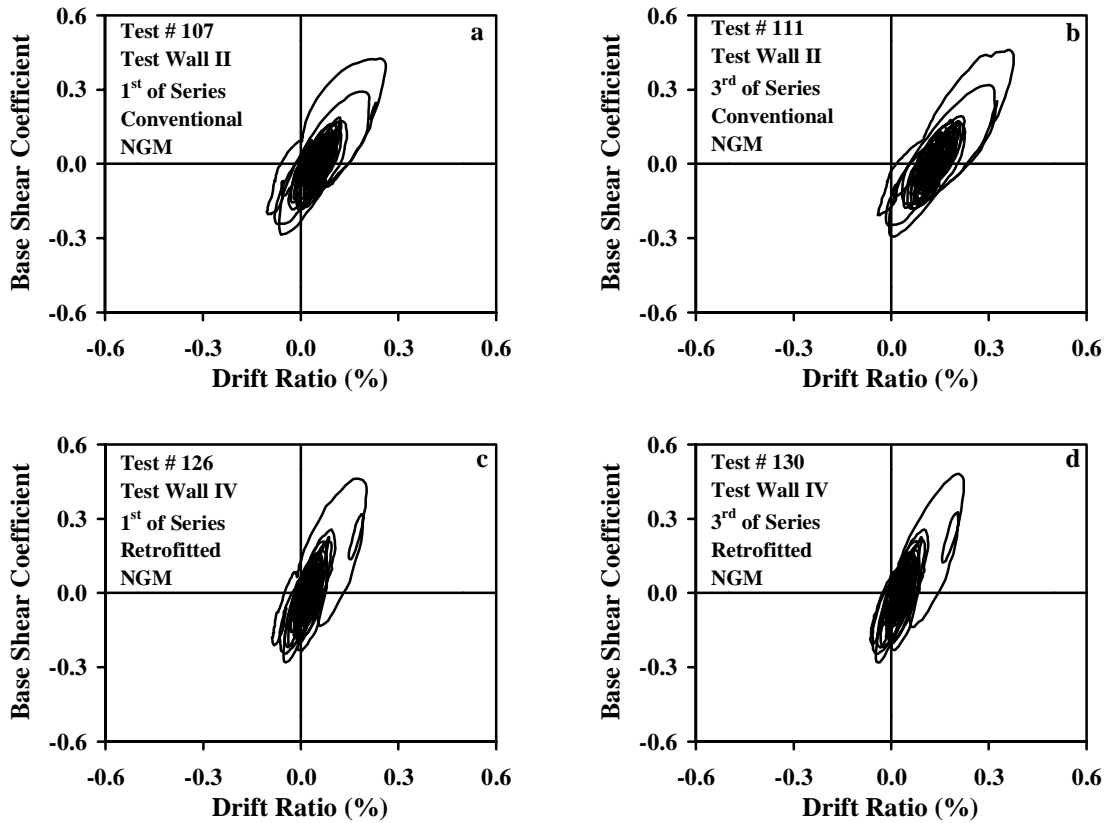


Figure 9 – Hysteresis Loops of Conventional and Retrofitted Walls Subjected to Near-Field Ground Motion (Seismic Loading II)

During the data analysis phase of this project, the hysteresis loop for the retrofitted shear wall was decomposed into its contributions from the wood framing system and the damper (due to space limitations, the decomposition is not shown here). Surprisingly, the damper hysteresis loop exhibited significant stiffness which was not consistent with the results from cyclic testing of the damper. Further analysis of the data revealed that the inconsistency was due to the deformation across the damper not being equal to the interstory drift of the wall due to: (i) construction tolerances (slack) that existed in the pinned connections at the ends of the damper and (ii) torsional response of the wall (see Figure 10). In spite of this inequality, the damper was effective in reducing the interstory drift of the retrofitted walls during seismic excitation. Note that the SDOF models of the shear wall, as defined by Eq. 2 and 4 for the conventional and retrofitted walls, respectively, are not accurate if there is slack in the system or twisting response occurs. However, the models may be regarded as reasonably accurate if the slack in the system and the twisting response are not excessive.

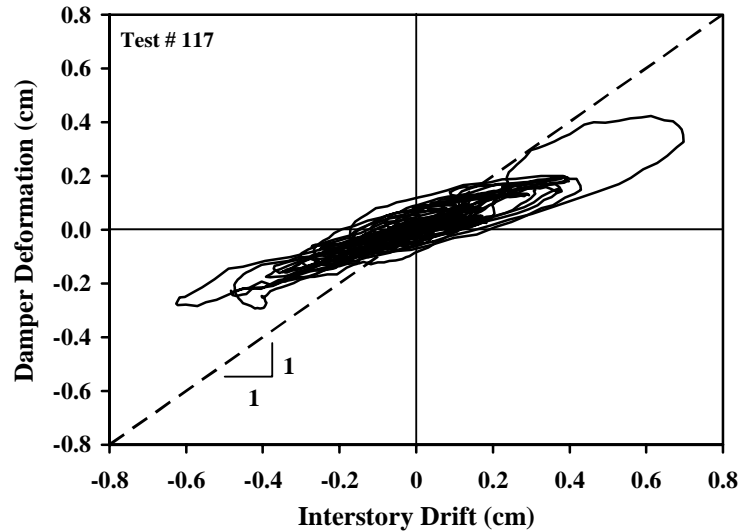


Figure 10 – Comparison of Interstory Drift and Deformation of Viscous Damper

CONCLUSIONS

The research presented herein evaluates the effectiveness of a supplemental fluid viscous damper installed within a light-framed wood shear wall subjected to both ordinary and near-field seismic ground motions. The effectiveness was evaluated via experimental shaking table tests of two conventional walls and two walls that were retrofitted with the supplemental viscous damper. One of each type of wall was subjected to a series of ordinary ground motions while the other two walls were subjected to a series of near-field ground motions.

The successful completion of the research demonstrates the feasibility of installing a fluid viscous damper within the dimensional restrictions of a conventional shear wall. Furthermore, the results of the research demonstrate the potential effectiveness of the viscous damper in mitigating seismic hazards. Specifically, the interstory drift and energy dissipation demand of the walls retrofitted with the viscous damper was reduced with respect to that of the conventional walls. The damper was most effective in improving the performance of the tested shear walls that had been subjected to prior seismic excitations.

The reduced interstory drift and energy dissipation demand on the retrofitted shear wall suggests that if the wall were located within a light-framed wood structure, damage, and thus financial loss, would be reduced during a seismic event. Further research is needed to evaluate: (i) the performance of retrofitted wood shear walls within three-dimensional structural systems; (ii) the effects of perforations in shear walls, and (iii) the influence of various structural and non-structural sheathing materials.

ACKNOWLEDGMENTS

The authors would like to thank Taylor Devices, Inc. of North Tonawanda, NY for donating the damper used in the experimental shaking table tests and for providing cyclic test data for the damper. In addition, the authors acknowledge Mr. Zhi Yi Huang, an undergraduate student, who assisted with construction of the test walls.

REFERENCES

1. Dinehart, D. W., Shenton, H. W. and Elliott, T. E. "The Dynamic Response of Wood-Frame Shear Walls with Viscoelastic Dampers." *Earthquake Spectra*, 1999; 15(1): 67-86.
2. Schierle, G.G. (Ed.) "Woodframe Project Case Studies." CUREE Report No. W-04, Consortium of Universities for Research in Earthquake Engineering (CUREE), Richmond, CA, 2001: pp. i-ii.
3. Filiatrault, A. "Analytical Predictions of the Seismic Response of Friction Damped Timber Shearwalls." *Earthquake Engineering and Structural Dynamics*, 1990; 19: 259-273.
4. Dinehart, D. W. and Shenton, H. W. "Comparison of the Response of Timber Shear Walls With and Without Passive Dampers." *Proc. of Structural Engineers World Congress*, San Francisco, CA, July, 1998; Paper T207-5.
5. Dinehart, D.W. and Lewicki, D.E. "Viscoelastic Material as a Seismic Protection System for Wood-Framed Buildings." *Proc. of 2001 Structures Congress and Exposition*, ASCE, Edited by P.C. Chang, Washington, D.C., May, 2001.
6. Higgins, C. "Hysteretic Dampers for Wood Frame Shear Walls." *Proc. of 2001 Structures Congress and Exposition*, ASCE, Edited by P.C. Chang, Washington, D.C., May, 2001.
7. Symans, M.D., Cofer, W.F., Fridley, K.J. and Du, Y. "Seismic Behavior of Wood-framed Structures with Viscous Fluid Dampers." *Earthquake Spectra*, 2004; 20(2), in press.
8. ICC. "International Building Code." International Code Council, Inc., Falls Church, VA, 2000.
9. Fischer, D., Filiatrault, A., Folz, B., Uang, C., and Seible, F. "Shake Table Tests of a Two-Story Woodframe House," CUREE Report No. W-06, Consortium of Universities for Research in Earthquake Engineering (CUREE), Richmond, CA, 2001.
10. Chopra, A.K. "Dynamics of Structures: Theory and Applications to Earthquake Engineering." Second Edition, Prentice Hall, Upper Saddle River, NJ, 2001.